World Academy of Science, Engineering and Technology
International Journal of Mechanical and Mechatronics Engineering
Vol:6, No:11, 2012

Experimental and Numerical Study of A/C Outlets and Its Impact on Room Airflow Characteristics

Mohammed A. Aziz, Ibrahim A. M. Gad, El Shahat F. A. Mohammed, and Ramy H. Mohammed

Abstract—This paper investigates experimental and numerical study of the airflow characteristics for vortex, round and square ceiling diffusers and its effect on the thermal comfort in a ventilated room. Three different thermal comfort criteria namely; Mean Age of the Air (MAA), ventilation effectiveness (E), and Effective Draft Temperature (EDT) have been used to predict the thermal comfort zone inside the room.

In experimental work, a sub-scale room is set-up to measure the temperature field in the room. In numerical analysis, unstructured grids have been used to discretize the numerical domain. Conservation equations are solved using FLUENT commercial flow solver. The code is validated by comparing the numerical results obtained from three different turbulence models with the available experimental data. The comparison between the various numerical models shows that the standard k-ε turbulence model can be used to simulate these cases successfully. After validation of the code, effect of supply air velocity on the flow and thermal field could be investigated and hence the thermal comfort. The results show that the pressure coefficient created by the square diffuser is 1.5 times greater than that created by the vortex diffuser. The velocity decay coefficient is nearly the same for square and round diffusers and is 2.6 times greater than that for the vortex diffuser.

Keywords—Ceiling diffuser; Thermal Comfort; MAA; EDT; Fluent; Turbulence model.

I. Introduction

NOWADAYS, the majority of people spend up to 90% of their time indoors. Knowledge and prediction of indoor climate conditions are important for optimizing indoor climate and thermal comfort, and it is also important for energy conservation [1-4]. Indoor air quality and thermal comfort are two important aspects of indoor environmental quality that receive considerable attention.

Design conditions of HVAC as specified by ASHRAE [5] are temperature, and relative humidity should be held in the range of (20-24oC), and 50% to 60%, respectively. Alongside, positive air pressure should be maintained, and all air exhausted with no recirculation is preferred [6].

The mean age of air (MAA) is one of the most important parameters describing the ventilation efficiency in a space. It is defined as the average time for air to travel from a supply outlet area to any location in a ventilated room [7-9]. Its concept is assumed to be equal zero (100% fresh) at inlet. It is obvious that the high values of MAA mean that part of the air circulates for a long time inside the room. So, the values of the MAA reflect the efficiency of ventilation system.

R. H. Mohammed is with the Zagazig University in Egypt (corresponding author to provide phone: 201114049331; e-mail: Rhamdy@ Zu.edy.eg).

Spitler [10] studied the effect of the inlet velocity on air distribution in a full scale unoccupied ventilated room has dimensions of 5m long, 3m wide, and 3m high. The supply and exhaust outlets are each 0.333m wide and 1.0m high. Nielsen [11] described experiments with wall-mounted air terminal devices. This study gave expressions for the velocity distribution close to the floor. The velocity at the floor was influenced by the flow rate to the room, the temperature difference and the type of the diffuser. Lobutova et al. [12] investigated the large-scale circulations of airflow in room with three dimensional particle tracking velocimetry (3D PTV). The 3D PTV system consisted of four CMOS cameras, two flash lamps, and an image recording and data processing system. In such study, velocity time series, probability density functions (PDF) of the velocity, and acceleration fluctuations had been calculated. Posner et al. [13] compared results from relatively simple three-dimensional numerical simulations (CFD) with Laser Doppler Anemometry (LDA) and Particle Image Velocimetry (PIV) experimental measurements of indoor air flows in a one-tenth sub-scale model room. The results of the numerical simulations and velocimetry measurements showed how the obstructions can greatly influence the air flow and contaminant transport in a room.

Al-Hamed [3] employed a computer program for simulating 3D room ventilation problems to predict the mean air temperatures and air velocities for a number of realistic supply air inlet and outlet locations. The k-ε turbulence model was considered. The flow field predicted by this model was validated by experimental measurements done by other investigator. His study showed that the PMV occupancy comfort response was more favorable.

Srebric and Chen [14] used a simplified method to describe flow and thermal information from eight various diffusers which were nozzle diffuser, slot (linear) diffuser, valve diffuser, displacement diffuser, round ceiling diffuser, square ceiling diffuser, vortex diffuser, and grille diffuser. The box method was suitable for most of the diffusers with an appropriate box size. The momentum method was applied well for five diffusers. Since the momentum method was simpler than the box method, the momentum method should be used, whenever it is applicable.

Zhou and Haghighat [15] developed a simplified method to define the boundary conditions at the inlet of the swirl diffuser. With this method a round diffuser was divided into six triangular sectors with equal air discharge rate, while various air throw orientation angles were assigned to each sector. Comparisons between smoke airflow visualization and CFD predictions demonstrated the effectiveness of the current

simplified modeling method of swirl diffuser. Profiles of temperature and air velocity from measurements were also presented to validate the CFD simulation results. This validation showed that the simplified method can be used to model the diffusers.

Einberga and Hagstrom [16] discussed the modeling results from CFD simulation of a multi-cone air diffuser for industrial spaces. CFD simulations were compared systematically with data from experimental measurements while air velocity was measured by ultrasonic sensors. The outcomes of this study showed that CFD simulation with a standard k–ε model accurately predicted non-isothermal airflow around the diffuser.

The majority of previous studies in indoor airflows were conducted in reduced scale rooms and the numerical simulations were compared to the reduced scale experiments. There was a lack of experimental data available to validate mathematical models. The turbulence model that more valid for different types of diffusers is not satisfied in the previous work. As a result, some fundamental issues remain unsolved related to the predictability of existing mathematical models for low Reynolds number flows. So, we will attempt to treat some of them.

In this study, the investigation of the characteristics of the indoor airflows is conducted through two approaches: experimental measurements and numerical simulations. The main objective of this study is to evaluate the performance of three ceiling diffusers and specify the more suitable turbulence model for these cases. Also, predict the region of the created thermal comfort.

II. Experimental Work

A. Experimental set-up

The general layout of the experimental set-up is shown in Fig. 1. It is consists of two main parts namely: air conditioning unit and test rig (model room).

The air conditioning unit is a simple vapor compression refrigeration cycle which used to deliver cold air to the test room. A fan pulls the atmospheric air and passing it over the evaporator. Cubic glassed model room is fabricated from Perspex having width, length, and height of 1x1x1 m. The round supply duct has 15 cm diameter that runs from an air conditioning discharging cold air to the inlet of the tested room.

The supply duct is fitted with discharge control gate in the form of the vortex diffuser which vanes can turn changing the air volume flow rate supplied to the room as shown in Fig. 2. The airflow enters the room from an opening at its ceiling of 15 cm diameter of which tested diffuser is installed.

The temperatures of floor, ceiling of the room, and air are measured by means of copper-constantan thermocouple (T-type). A sliding arm having fixed thermocouple at its terminal end is installed at the corner of the room, it can move along three dimensions to measure the temperature inside the room (Fig. 1). Thermocouple is fixed just before the outlet diffuser to measure the inlet temperature. Alongside, other thermocouples are mounted on the four walls, floor and on the roof. All thermocouples are connected to switches and digital thermometer. The thermocouples readings are measured from digital thermometer which has uncertainty of ± 0.2°C of received readings.

Digital manometer is used to measure the air velocity (V_d) before the diffuser and hence, the volume flow rate can be then predicted. The error of the measured value is about ± 0.1 m/s. Based on measured air velocity, the air flow rate can be determined. The pressures drop a cross orifice meter is measured by using inclined water manometer having error about ± 0.1 mm H2O. It should be noted that the calibration of the above instruments are a very important task that should be carried out in this type of tests.

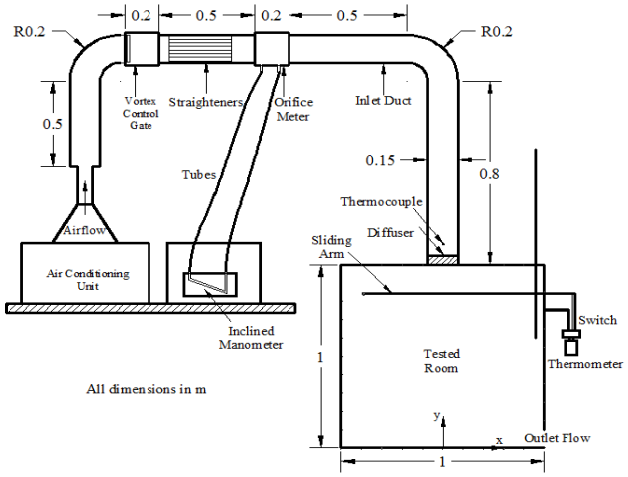

Fig. 1 Schematic diagram of the present experimental model room

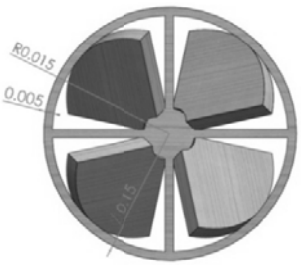

Fig. 2 Vortex control gate

B. Uncertainty Estimation

The compound variables such as air density, discharge flow coefficient, and ventilation effectiveness can be calculated as follows:

The uncertainty associated with air density (Uρ) can be written as:

$$U_\rho = \frac{\partial \rho}{\partial T} U_T \quad (1)$$

The uncertainty associated with discharge flow coefficient (UCd) can be written as:

$$U_{C_d}{}^2 = \left[\left(\frac{\partial C_d}{\partial V_d} U_{V_d}\right)^2 + \left(\frac{\partial C_d}{\partial \rho} U_\rho\right)^2 + \left(\frac{\partial C_d}{\partial \Delta H} U_{\Delta H}\right)^2\right] \quad (2)$$

The uncertainty associated with ventilation effectiveness (UE) can be written as:

$$U_E{}^2 = \left[\left(\frac{\partial E}{\partial t_s}U_{t_s}\right)^2 + \left(\frac{\partial E}{\partial t_m}U_{t_m}\right)^2 + \left(\frac{\partial E}{\partial t_e}U_{t_e}\right)^2\right] \quad (3)$$

The results of this analysis are summarized in Table I.

TABLE I
UNCERTAINTY OF COMPOUND VARIABLE

Compound Variable	Uncertainty (%)
Air Density	0.066
Discharge flow coefficient	2.245
Ventilation effectiveness	6.88

C. Experimental Procedure

In the present work, mainly three types of ceiling diffusers are involved. These diffusers are namely: vortex (swirl), round, and square ceiling diffusers. Each diffuser is installed and investigated sequentially. For each diffuser, the various inlet air temperatures in range from 18 to 24°C and volume flow rates are adjusted to study its effects on the airflow characteristics. The range of the studied inlet air velocity is from 1 to 4 m/s.

The model room is prepared and adapted to the conditions to the investigated cases. Zero readings of all instruments should be settled. The air conditioning unit is switched on so that the cold air is to be supplied to the room through the supply inlet duct. The air flow rate is then adjusted by means of the vortex control gate.

On achieving the steady state conditions, a number of temperatures are carried out subsequently averaged. The number of successive measurements depends on the degree of steadiness of the temperature. The system is allowed time to stabilized after each adjustment. It is considered steady state when temperatures agreed within 2% between two consecutive readings taken every 5 min. The steady state has been observed about 15 min. After achieving the steady state, the pressure drop across orifice meter, the room air inlet temperature, and T-type thermocouple readings inside the room are recorded. These procedures are then repeated through succession value of the input flow rate of the supply air.

III. NUMERICAL MODEL

The numerical study is conducted to simulate the airflow in a sub-scale room. The steady, viscous, 3D governing equations, and the mean age of air transport equation representing the flow field are solved. The FLUENT package includes FLUENT 6.3.26 [17] and GAMBIT 2.4.6 are used to simulate the problem under this consideration. Indoor airflow calculations use the Boussinesq approximation for thermal buoyancy [18]. The approximation takes air density as constant in the momentum terms and considers the buoyancy influence on air movement by the difference between the local air weight and the pressure gradient. With an eddy-viscosity model, the indoor airflow is described by the following time-averaged Navier-Stokes equations for the conservation of mass, momentum, energy, and species transport equation [19-21].

- *Continuity Equation*

$$\frac{\partial V_i}{\partial x_i} = 0 \quad (4)$$

where Vi= mean velocity component in xi-direction; xi = coordinate (for i =1, 2, 3, xi corresponds to three perpendicular axes).

- *Momentum Equation*

$$\frac{\partial \rho V_i}{\partial t} + \frac{\partial \rho V_i V_j}{\partial x_j} = -\frac{\partial P}{\partial x_i} + \frac{\partial}{\partial x_j}\left[\mu_{eff}\left(\frac{\partial V_i}{\partial x_j} + \frac{\partial V_j}{\partial x_i}\right)\right] + \rho\beta(t_o - t)g_i \quad (5)$$

where ρ= air density; Vj = velocity component in xj-direction; P = pressure; μeff = effective dynamic viscosity; β = thermal expansion coefficient of air; to = temperature of a reference point; t= temperature; gi = gravity acceleration in i-direction. The last term on the right side of the Eq. (2) is the buoyancy term. The turbulent influences are lumped into the effective viscosity as the sum of the turbulent viscosity μt and laminar viscosity μl:

$$\mu_{eff} = \mu_t + \mu_l \quad (6)$$

- *Energy Equation*

The energy equation describes the temperature distribution throughout the non-isothermal flow domain. This equation is derived from the first law of thermodynamics to the elemental central volume as following [3]:

$$\frac{\partial(\rho C_p u_j T)}{\partial x_j} = \frac{\partial}{\partial x_j}\left(\lambda_{eff}\left(\frac{\partial T}{\partial x_j}\right)\right) + S_T \quad (7)$$

where Cp is the specific heat at constant pressure (J/kg.°C), ST is the source term (W/m3), and λeff is the effective thermal conductivity (W/m.°C) which can be expressed as,

$$\lambda_{eff} = \lambda_l + \lambda_t \quad (8)$$

where λl is the laminar thermal conductivity and λt is the turbulent thermal conductivity which depends on the local flow field.

- *Concentration of species equation*

$$\frac{\partial \rho V_j C}{\partial x_j} = \frac{\partial}{\partial x_j}\left[\Gamma_{c,eff}\left(\frac{\partial C}{\partial x_j}\right)\right] + Sc \quad (9)$$

where C is species concentration; $\Gamma_{c,eff}$ is effective turbulent diffusion coefficient for C; SC is source term of C. Similar method to the energy equation is used to determine the effective diffusive coefficient for species concentration $\Gamma_{C,eff} = \frac{\mu_{eff}}{Sc_{eff}}$ where effective Schmidt number, Sceff, is equal to 1.0.

- *Standard k-ε model*

$$\frac{\partial}{\partial x_i}(\rho u_i k) = \left(\mu + \frac{\mu_t}{\sigma_k}\right)\nabla^2 k + \mu_t S^2 - \rho\varepsilon \quad (10)$$

$$\frac{\partial}{\partial x_i}(\rho u_i \varepsilon) = \left(\mu + \frac{\mu_t}{\sigma_\varepsilon}\right)\nabla^2 \varepsilon + C_{\varepsilon 1}\frac{\varepsilon}{k}\mu_t S^2 - C_{\varepsilon 2}\rho\frac{\varepsilon^2}{k} \quad (11)$$

$$\mu_t = \frac{\rho C_\mu k^2}{\varepsilon} \quad (12)$$

The coefficients are (C_μ, σ_k, σ_ε, $C_{\varepsilon 1}$, $C_{\varepsilon 2}$) = (0.09, 1.0, 1.3, 1.44, 1.44) and $S=(S_{ij}S_{ij})^{0.5}$.

The thermal comfort indices which used in this study can be calculated as following:

- *Mean age of the air (MAA)*

The mean age of air can be calculated from the following transport equation:

$$\frac{\partial}{\partial x}\left(\rho u_i \mathrm{MAA} - \left(2.88\rho \times 10^{-5} + \frac{\mu \mathrm{eff}}{0.7}\right)\frac{\partial MAA}{\partial x_i}\right) = S \quad (13)$$

where S is the source term, which depends on the density of the air mixture [7, 8].

The MAA is not directly available from Fluent so, it is programmed and calculated as user-defined scalars.

- *Overall ventilation effectiveness (E)*

The overall ventilation effectiveness represents the effectiveness of energy utilization supplied into the occupied zone to achieve a satisfactory thermal comfort level [9].

$$E = \frac{t_e - t_s}{t_m - t_s} \text{ x100} \quad (14)$$

- *Effective draft temperature (EDT)*

The EDT index is combination of temperature and air velocity. The values of the effective draft temperature between -1.7 and 1.1 characterize the thermal comfort [1]. Values less than -1.7 represent cool sensation while values above 1.1 represent warm sensation. This expression for EDT is given by:

$$EDT = (t_x - t_m) - 8(V_X - 0.15) \quad (15)$$

Fig. 3 shows the computational domain which consists of four walls, ceiling, and floor. Each has 1m height and 1m width and outlet opening is of 0.17m width and 0.1m height. Vortex, square, and round diffusers (manufactured by TROX) are simulated. Each diffuser has 15cm neck diameter is conducted into the computational domain in order to study its effect on the airflow characteristics.

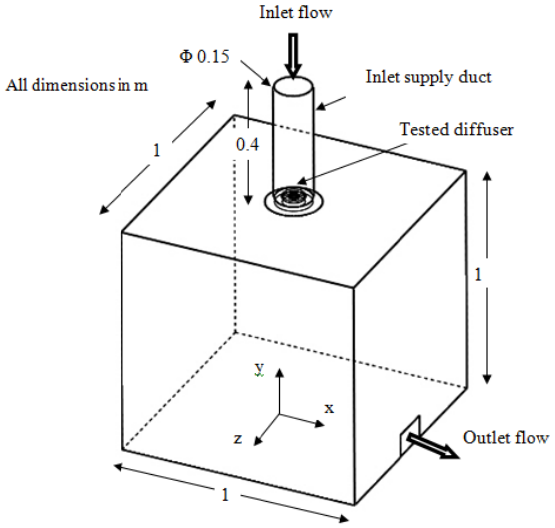

Fig. 3 Computational domain

a- Mesh Sensitivity

Several unstructured grids are performed with different mesh sizes for each diffuser in order to guarantee the grid independence of the results. Fig. 4 shows the temperature and velocity distribution respectively over vertical line at the center of the room for 37000 (37k), 87000 (87k), 115000 (115k), and 150000 (150k) grid sizes. In this graphs, the obtained results with 115k and 150k are very close where the maximum percentage error is about 0.4%. Therefore, the results from 150 k grid size can be considered to be grid independence.

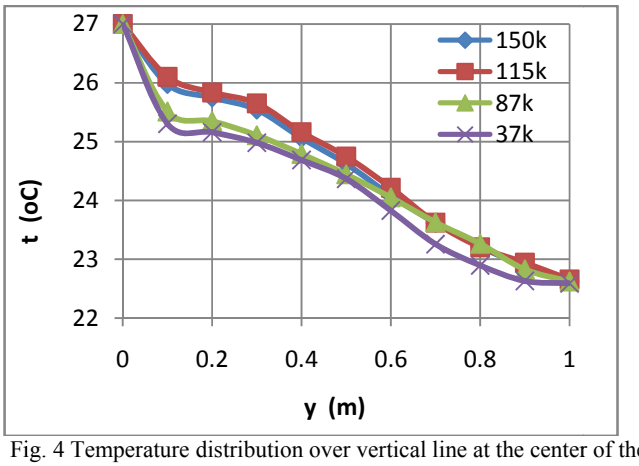

Fig. 4 Temperature distribution over vertical line at the center of the room - vortex diffuser

IV. Code Validation

One case of the vortex diffuser with 45o swirling angle is selected to establish the validation process where the three different types of the turbulence models namely; standard k-ε, RNG k-ε, and standard k-ω are investigated. A comparison between the predicted results by the numerical code using commonly used three turbulence models specified for indoor airflow simulation, the present experimental data, and the previous measurements by Srebric [14] is performed.

Fig. 5 shows the comparison between the predicted temperature distributions by FLUENT for the three turbulence models and the present measured temperature over the vertical line. This figure shows similar trends of the compared data.

Fig. 6 shows the comparison between the vertical dimensionless velocity distributions (V/V_o) obtained from the three considered turbulence models and the Srebric's measurements. Also, both the square and round diffuser create same trend. Accordingly, the standard k-ε turbulence model can be used to simulate indoor airflow with good agreement.

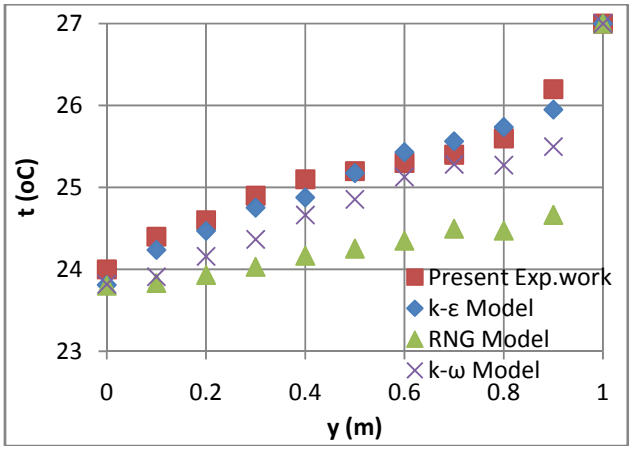

Fig. 5 Temperature distribution measured by present work and predicted by three types of turbulence models - vortex diffuser

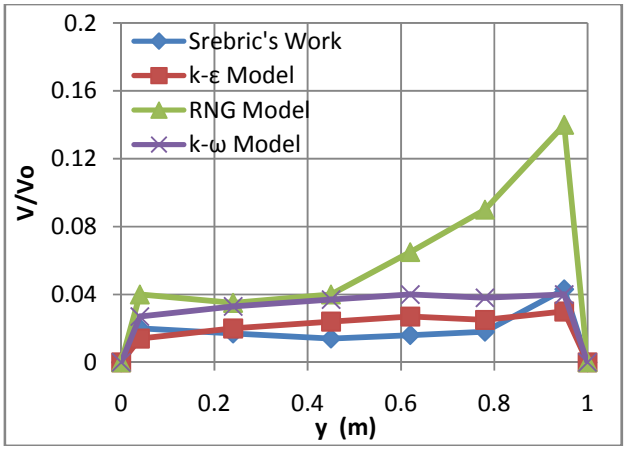

Fig. 6 Comparison between (V/V_o) distribution measured by Srebric [14] and predicted by three types of turbulence models - vortex diffuser

V. Results and Discussion

a- Description of Air Flow emerged from the Ceiling Diffusers

Fig.7a presents the path lines exit from the vortex diffuser with 45° swirling angle. The swirling jet flow from the diffuser reaches to the middle of the room. The throw of the diffuser seems as a short and the swirl flow diminishes at the middle height of the room therefore, there is no vortex or swirl flow on the lower half of the room (occupied zone). In the same way, the flow of the round diffuser emerges radically and reaches to the side walls then it turns 90° downward and a vortex ring is create near the ceiling. The throw of the round diffuser is noticeably longer as shown in Fig. 7b. This figure shows that the emerged air jet from the square diffuser has two dimensions without any swirling flow. The velocity vectors from the square diffuser are shown in Fig. 7c. The throw of the diffuser seems a long where the flow just reaches to the side walls. After the flow reaches to the wall, it turns 90° downward, where two vortexes create the next to the vertical walls and the ceiling in the upper corner of the room.

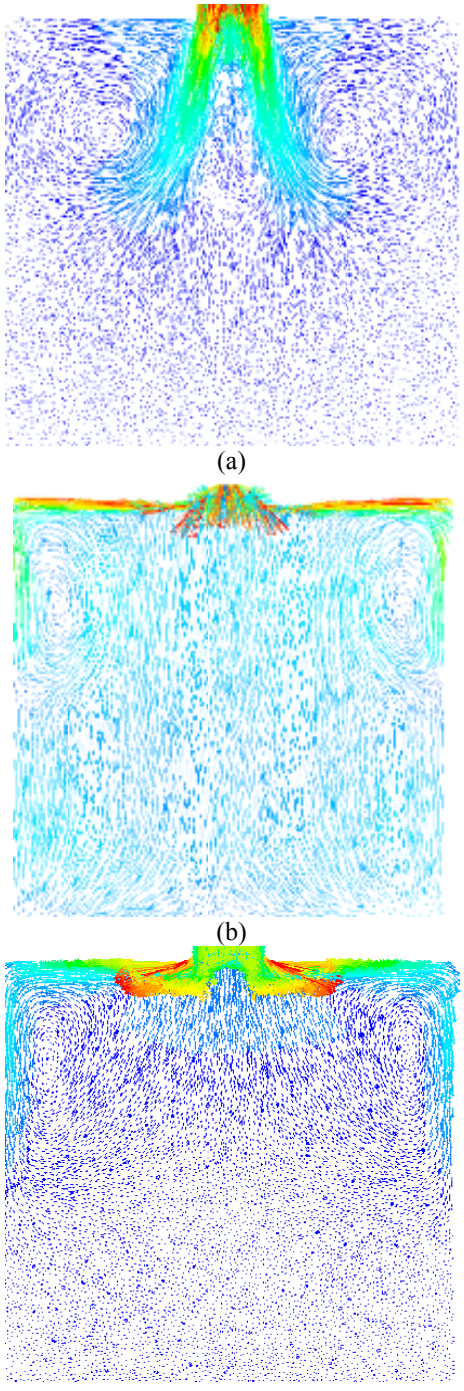

(a)

(b)

(c)

Fig. 7 Velocity vector at the vertical plane for (a) vortex, (b) round, and (c) square diffuser

b- Effect of the inlet velocity

Fig. 8 shows the relationship between the pressure coefficient and Reynolds number for the three diffusers. Both pressure coefficient and Reynolds number can be calculated from Eq. (16) and Eq. (17) respectively.

$$Cp = \frac{\Delta P}{\frac{1}{2}\rho V^2} \quad (16)$$

$$Re = \frac{\rho V d}{\mu} \quad (17)$$

From Fig.8, it is clear that all three tested diffusers have the same trend. The highest values of Cp are belonging to the square diffuser while the minimum values are belonging to the vortex one.

The dimensionless mean velocity V_m/V_o is plotted with the Reynolds number Re as in Fig. 9. From this figure, it is clear that the dimensionless mean velocity V_m/V_o increases with Reynolds number in case of the round diffuser only.

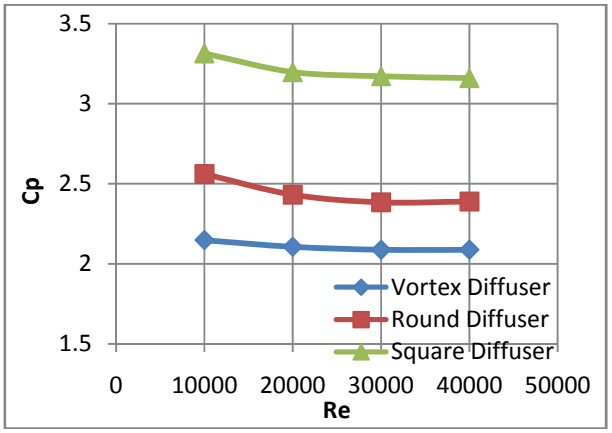

Fig. 8 Pressure coefficient at different Reynolds number for different diffusers

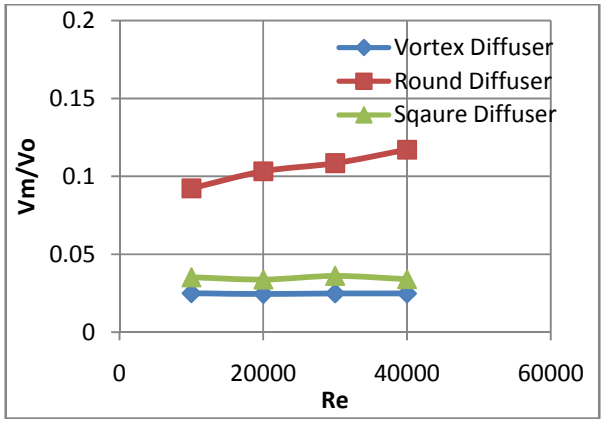

Fig. 9 Dimensionless mean velocity at different Reynolds numbers for different diffusers at same inlet temperature and relative humidity

Fig. 10 shows the effect of the Reynolds number on the dimensionless mean temperature. The room seems as cool in case of the vortex diffuser because the cold air jet from the vortex diffuser is focused and concentrated on the middle of the room.

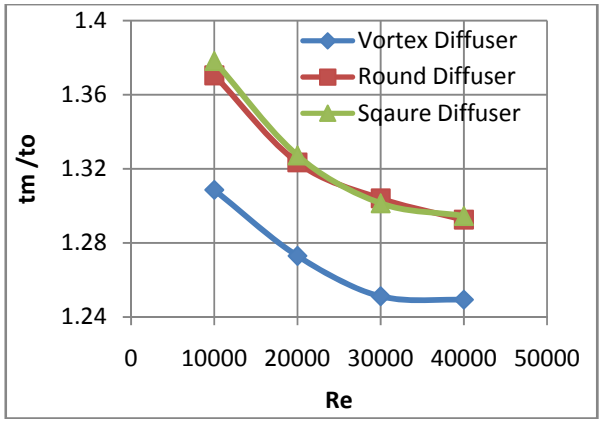

Fig. 10 Dimensionless mean room temperature at different Reynolds numbers for different diffusers at same inlet temperature and relative humidity

Fig. 11 shows the relation between the dimensionless mean relative humidity in the room and Reynolds number. As the air inlet velocity increases by 1m/s, the mean value of the relative humidity in the room increases by about 2%. This can be explained referring to Fig. 10 where the vortex diffuser demonstrates the highest value of the dimensionless mean relative humidity because it has the lowest room temperature while the value of the square and the round diffuser is nearly same.

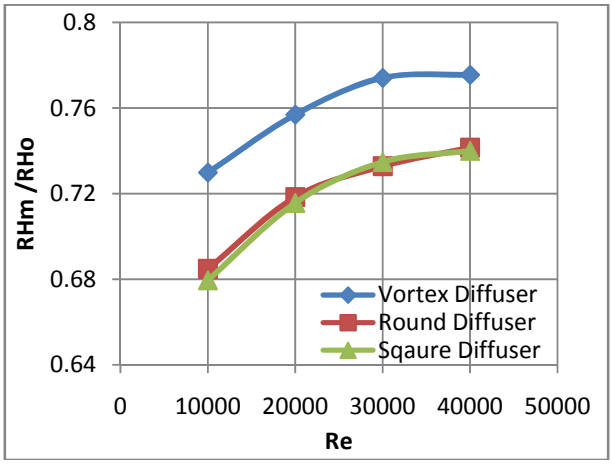

Fig. 11 Dimensionless mean room relative humidity at different Reynolds numbers at same inlet temperature and relative humidity

Fig. 12 shows the mean effective draft temperature within the room at different inlet velocities for the three studied diffusers. From this figure, it can be seen that, as the inlet velocity increases, the mean value of the effective draft temperature decreases and vice verse. The vortex diffuser demonstrates the highest values where the round diffuser demonstrates the lowest one at Reynolds number over 30,000 out of the comfort zone.

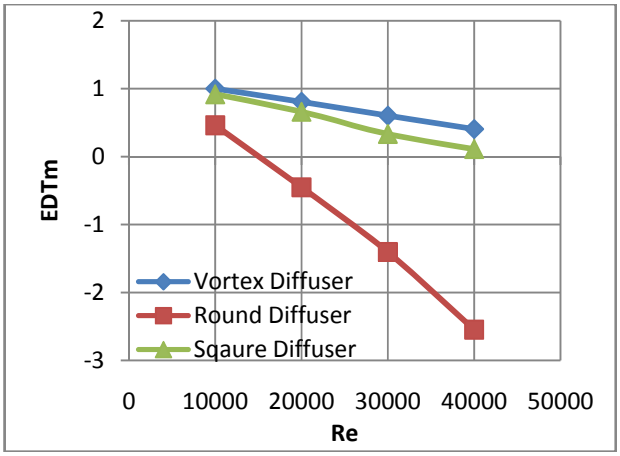

Fig. 12 Mean effective draft temperature in room at different Reynolds numbers

Fig.13 shows the distribution of the mean age of the air in the room for the three considered diffusers. From this figure, it can be seen that the maximum values of the mean age of the air in case of the vortex and round diffuser is nearly the same and larger than the square diffuser. This can be attributed to the buoyancy force raises the flow upward and it has a great effect on the path lines of the air inside the room. The stratification of the MAA is well established velocity in case of the square diffuser.

The lower values of the mean age of the air don't allow the air to exchange the heat with the walls. This means that the air is extracted from the room with low temperature. Hence, the ventilation effectiveness for the square diffuser is small as shown in Fig. 14. This in turn results in the highest ventilation effectiveness for the round diffuser.

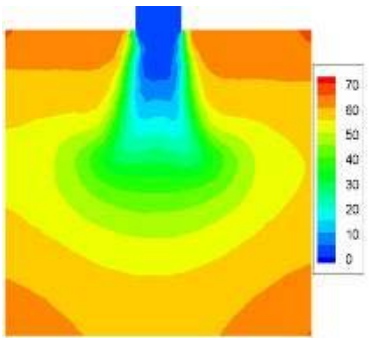

(a)

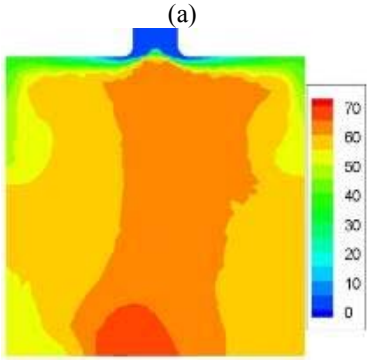

(b)

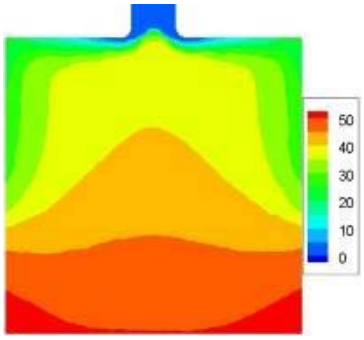

(c)

Fig. 13 Mean age of the air distribution in sec for (a) vortex, (b) round, and (c) square diffuser

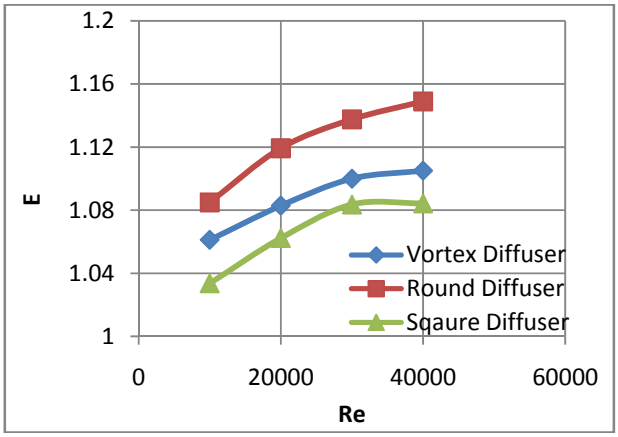

Fig. 14 Ventilation effectiveness at different Reynolds number at same inlet temperature and relative humidity for studied diffusers

c- Diffuser velocity decay coefficient

The performance of the jet created by the diffuser can be characterized by a single constant, namely jet velocity decay coefficient (K value). The jet velocity decay coefficient can be defined as [22]:

$$\frac{V}{V_o} = K\frac{\sqrt{A_o}}{x} \quad (18)$$

The diffuser velocity decay coefficient (K) can be determined by plotted the dimensionless velocity versus the dimensionless distance (x/√Ao) as shown in Fig. 15 where the values of the decay coefficient can be directly determined when the curve intersects the dimensionless velocity at the unity (i.e. V/Vo =1) as outlined in reference [22]. The values of the velocity decay coefficient are tabulated in Table II.

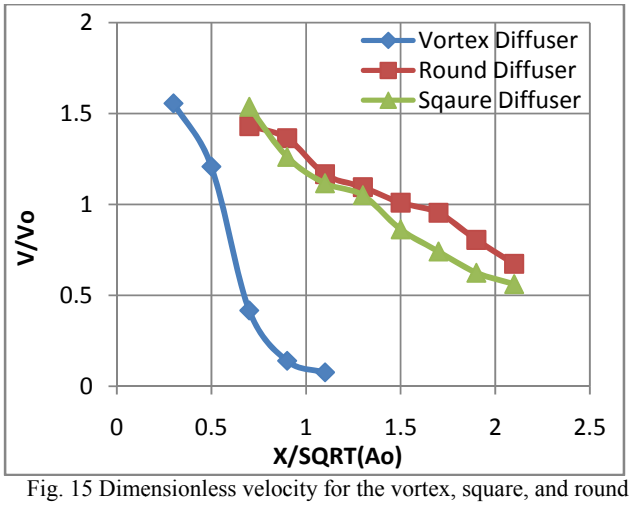

Fig. 15 Dimensionless velocity for the vortex, square, and round diffusers

TABLE II
VELOCITY DECAY COEFFICIENT FOR THE THREE TESTED CEILING DIFFUSERS

Diffuser type	Velocity decay coefficient
Vortex	0.57
Square	1.4
Round	1.5

d- Swirling angle of the vortex diffuser

The swirling angle is the inclination of the diffuser blades on the vertical plane. The effect of three values of swirling angle namely 30°, 45°, and 60° are investigated where the inlet velocity is 1 m/s, the inlet temperature is 18°C, the isothermal walls at 28.5°C, and the isothermal ceiling at 27°C.

Fig. 16 shows that the inclination angle of 60° has the longest throw but it has high pressure coefficient (Cp) as tabulated in Table III.

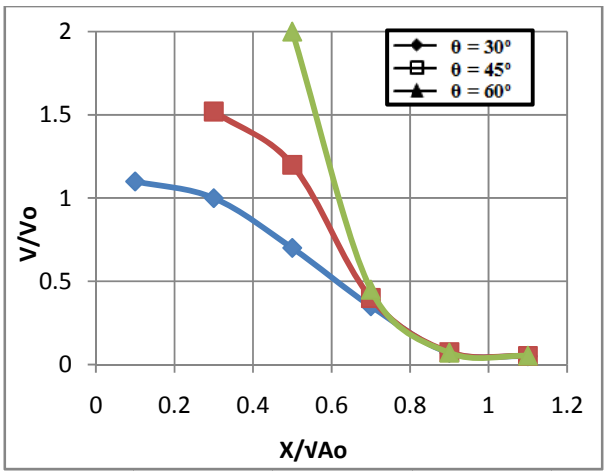

Fig. 16 Dimensionless velocity for different swirling angles for vortex diffuser

TABLE III
VELOCITY DECAY COEFFICIENT FOR VORTEX DIFFUSER

Swirling Angle	K	C_p
30°	0.3	0.88
45°	0.57	2.20
60°	0.61	7.65

VI. CONCLUSION

A new set of the experimental and numerical investigation to study the performance of the vortex, round, and square ceiling diffusers has been reported for various inlet temperature, velocity, and relative humidity. The results of this study can be summarized as follows:

- The produced results of the standard k-ε turbulence model are fully compatible with the measurements of temperature and flow field hence, it can be used to simulate the vortex, square, and round ceiling diffusers.
- The velocity vector of the vortex ceiling diffuser exhibits three specified regions namely: main swirling stream regions of the primary flow, upper recirculation region at the end of the jet, and lower region without any recirculation or swirling flow.
- The buoyancy force has great effect on temperature and velocity field, and the thermal comfort zone created by the three diffusers is large and wide but diminished when the inlet air velocity increases for the round diffuser.
- The air passing area of the vortex diffuser is higher than that of the round and the square diffusers at the same neck area. The pressure coefficient created by the square diffuser equals to 1.5 times greater than that created by the vortex diffuser.
- The velocity decay coefficient is nearly the same for square and round diffusers and equals to 2.6 times for the vortex diffuser.
- The inclination (swirling) angle of 60° has the best performance followed by the inclination angle of 45° but the inclination angle of 45° is preferable because it has low pressure drop, thus it is suitable for the high buildings due to its small throw and its jet is focused on the room center.

REFERENCES

[1] A. F. Alfahaid, Effects of ventilation on human thermal comfort in rooms, Ph. D Thesis, old dominion university, Norfolk, Virginia, 2000.
[2] A. H. Al-Hamed, Determining Velocity, Temperature and Occupancy Comfort within a 3-D. Room, M.A. Thesis, King Fahd University, Saudi Arabia, 1990.
[3] S. A. Al-Sanea, M. F. Zedan, and M. B. Al-Harbi, "Effect of supply Reynolds number and room aspect ratio on flow and ceiling heat transfer coefficient for mixing ventilation", International Journal of Thermal Sciences, vol. 54, pp. 176-187, 2012.
[4] H. B. Awbi, Ventilation of Buildings, Second edition, Spon Press, 2003.
[5] ASHRAE Handbook. Fundamentals, 2008.
[6] ASHRAE Standards, Standard 55, 1992.
[7] J. Abanto, D. Barrero, M. Reggioa, and B. Ozell, "Airflow modeling in a computer room", Building and Environment, Vol. 39, pp. 1393-1402, 2004.
[8] M. Bartak, M. Cermak, J. A. Clarke, J. Denev, F. Drkal, M. Lain, I. A. Macdonald, M. Majer, and P. Stankov, "Experimental and numerical study of local mean age of air", seventh International IBPSA Conference, Rio de Janeiro, Brazil, August 13-15, 2001.
[9] G. Gan, "Evaluation of room air distribution systems using computational fluid dynamics", Energy and Buildings, Vol. 23, pp. 83-93, 1995.
[10] J. D. Spitler, An experimental investigation of air flow and convective heat transfer in enclosures having large ventilative flow rates, Ph.D. Thesis, University of Illinois at Urbana-Champaign, 1990.
[11] P. V. Nielsen., "Velocity distribution in a room ventilated by displacement ventilation and wall-mounted air terminal devices", Energy and Buildings, Vol. 31, no. 3, pp. 179-187, 2000.

[12] E. Lobutova, C. Resagk, and T. Putze, "Investigation of large scale circulations in room airflows using three-dimensional particle tracking velocimetry", Building and Environment, Vol. 45, pp. 1653-1662, 2010.
[13] J. D. Posner, C. R. Buchanan, and D. Dunn-Rankin, "Measurement and prediction of indoor air flow in a model room", Energy and Building, Vol. 35, pp. 515-526, 2003.
[14] J. Srebric, and Q. Chen, "Simplified numerical models for complex air supply diffusers", HVAC&R Research, Vol. 8(3), pp. 277-294, 2002.
[15] L. Zhou, and F. Haghighat, "simplified method for modeling swirl diffusers", Department of Building, Civil and Environmental Engineering Concordia University, Montreal, Canada, 2007.
[16] G. Einberga, and Hagstrom K.," CFD modeling of an industrial air diffuser predicting velocity and temperature in the near zone", Building and Environment, Vol. 40, pp.601–615, 2005.
[17] Fluent Inc., User's Guide for Fluent/UNS, Release 6.3, Lebanon, USA, 2006.
[18] S. C. Hu, "Airflow characteristics in the outlet region of a vortex room air diffuser, Building and Environment, Vol. 38, pp.553-561, 2003.
[19] J. L. Lumley, and Tennekes H., A First Course in Turbulence, MIT Press, London, England, 1972.
[20] T. B. Gatski, Hussaini M. Y., and Lumley J. L., Simulation and Modeling of Turbulent Flows", New York, Oxford, Oxford University Press, 1996.
[21] J. H. Ferziger, and Peric M., Computational Methods for Fluid Dynamics. Springer Verlag, Berlin, Germany, 1996.
[22] Shakerin S., and Miller P. L., "Experimental study of vortex diffusers, University of the Pacifica", November 1995.